



1 **Reduction Evaluation and Management of Agricultural Non-Point**  
2 **Source Pollutant Loading in the Huntai River Watershed in**  
3 **Northeast China**

4 YiCheng Fu\*, Wenqi Peng, Chengli Wang, Jinyong Zhao, Chunling Zhang  
5 *State Key Laboratory of Simulation and Regulation of River Basin Water Cycle, China Institute*  
6 *of Water Resources and Hydropower Research*

7 \* Corresponding author, E-mail: [swfyc@126.com](mailto:swfyc@126.com)

8

9 **Abstract:**

10 With the raise of environmental protection awareness, applying models to control NPS  
11 (non-point source) pollution has become a key approach for environmental protection and  
12 pollution prevention and control in China. In this study, we implanted the semi-conceptual  
13 model SWAT (Soil and Water Assessment Tool) using information on rainfall runoff, land use,  
14 soil and slope. The model was used to quantify the spatial loading of NPS nutrient total nitrogen  
15 (TN) and total phosphorus (TP) to the Huntai River Watershed (HTRW) under two scenarios:  
16 without and with projected buffer zones of approximately 1 km within both banks of the Huntai,  
17 Taizi and Daliao river trunk streams and 5 km around the reservoirs. Current land-use types  
18 within the buffer zone were varied to indicate the natural ecology and environment. The Nash-  
19 Sutcliffe efficiency coefficient ( $E_{NS}$ ) and  $R^2$  for flow and predicted nutrient concentrations (TN  
20 and TP) in a typical hydrological station were both greater than 0.6, and the relative deviation  
21 ( $|Dv|$ ) was less than 20%. Under the status quo scenario (SQS), the simulated soil erosion in the  
22 HTRW per year was 811 kg/ha, and the output loadings of TN and TP were 19 and 7 kg/ha,  
23 respectively. The maximum loadings for TN and TP were 365 and 260 kg/ha, respectively.



24 Under environmental protection scenarios (EPS), the TN and TP pollutant loadings per unit  
25 area were reduced by 26% and 14% annually, respectively. Loading analysis showed that land-  
26 use type is a key factor controlling NPS pollution. The NPS pollutant loading decreased under  
27 the simulated EPS, indicating that environmental protection measures may reduce the NPS  
28 pollutant loading in HTRW. The 22% pollutant reduction under the EPS. We finally quantified  
29 the ratio of the land area lost to agricultural production compared with that lost to ecosystem  
30 services. We calculated the agricultural yield elasticity and concluded that the corresponding  
31 crop yield would be reduced by 2% when the land area for ecosystem services in the basin  
32 increased by 1% under the EPS.

33 **Keywords:**

34 Agricultural Non-Point Source pollutant loading; Environmental Protection Scenarios; Agro-  
35 ecosystem services; Huntai River Watershed

36 **1. Introduction**

37 The non-point source (NPS) pollution strongly influences soil restoration, people living  
38 environments and water quality safety. Many articles have indicated that underlying surface  
39 conditions and rainfall features will affect the spatial distribution characteristics of NPS  
40 pollution nutrient loading (Robinson et al.,2005). Pollutant loadings from different land-use  
41 types vary significantly (Niraula et al.,2013). The NPS pollutant concentration in water depends  
42 on the discharge loading and pollutant treatment rate. Presently, a lot of academics prefer  
43 loadings over concentrations to express their study (Yang et al., 2007; Ouyang et al.,2010;  
44 Outram et al., 2016). Land-use types and underlying surface status will impact the nutrient  
45 resources and spatial distribution characteristics (Ahearn et al., 2005; Ouyang et al., 2013). The  
46 spatial-temporal characteristics of NPS pollutants can be studied based on panel data statistical



47 analysis and multi-model simulation. The SWAT model can be implemented for NPS pollutant  
48 loading and provide the optimization programme for comprehensive ecological protection of  
49 watershed (Shen et al.,2011). A large number of literatures have demonstrated that combining  
50 different land use scales, land coordinated development patterns and geomorphologic landscape  
51 characteristics can decrease NPS pollution loadings (Sadeghi et al.,2009).

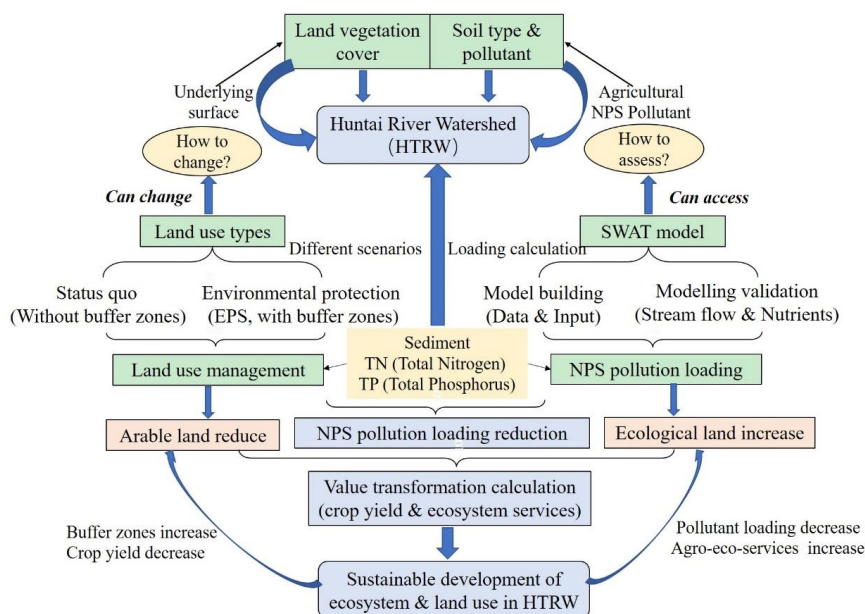
52 Distributed physically-based and semi-conceptual models can effectively calculate and  
53 evaluate NPS pollution loading spatial layouts. In the late 20<sup>th</sup> century, American scientists at  
54 United States Department of Agriculture-Agricultural Research Service (USDA-ARS)  
55 developed the SWAT model (Arnold et al.,1998), which has been widely used to simulate  
56 runoff, estimate NPS pollution loading and implement Best Management Practices (BMPs).  
57 SWAT is comprehensively used in evaluating the influence of NPS pollution loading on  
58 different regional natural landscape characteristics and land-use types, including vegetation  
59 coverage, underlying surface, agricultural generation modules and hydrometeorology data. The  
60 changes of agricultural NPS contaminations based on the diversification of land development  
61 types have been analyzed and researched by SWAT models (Ficklin et al.,2009; Shen et al.,  
62 2013). The SWAT model's main body contains 701 mathematical equations and 1013  
63 intermediate variables, which have been widely used to determine and evaluate NPS pollutant  
64 loading spatial distribution characteristics to quantitative the impacts of land use on NPS  
65 pollutants and soil-water loss sensitive evaluation on a watershed scale (Gosain et al.,2005;  
66 Ouyang et al., 2009; Logsdon et al.,2013).

67 HTRW is the basic product manufacturing base in China and a primary tributary of the Liaohe  
68 River Basin, which has been heavily polluted in recent years. The main NPS pollution in the  
69 Liaohe river is agricultural NPS pollution, and most NPS pollution occurs in the HTRW within



70 Liaoning province (Liaoning Province DEP, 2011). Therefore, the HTRW faces enormous  
71 pressure from water pollution risk. The annual mean growth of Gross Domestic Product (GDP)  
72 in the Liaohe River Basin was more than 13%, and the urbanization rate was almost 75%. The  
73 policy of ‘Revitalization of Old Industrial Bases in Northeast China’ has caused great spatial  
74 pattern changes to the land-use (Liu et al.,2014). This accelerating urbanization changes the  
75 current land use in a way that results in more NPS pollution to local surface waters.

76 The SWAT model was applied to quantify the TN and TP output loading in HTRW under  
77 different land uses, assess the NPS pollutant loading reduction, and analyse the spatial  
78 distribution characteristics under the condition of land cover change. Using SWAT, nutrient  
79 losses were simulated and evaluated under two scenarios: the status quo scenario (SQS, without  
80 buffer zones) and the ‘environmental protection’ scenario (EPS, with buffer zones). We studied  
81 NPS pollution problems in HTRW according the following steps and illustrated in the Fig. 1:  
82 (1) define the underlying surface (land-use) status for HTRW; (2) implement a SWAT model  
83 to simulate the NPS pollution loading (TP and TN) of the HTRW under two scenarios; (3)  
84 compare the NPS pollution loading under the two scenarios and assessed the effect of reducing  
85 pollutant loading under EPS; and (4) analysed the correlation between arable land area  
86 decrease/agro-ecosystem services increase and crop yield reduction using a simple static model.



87

88 **Fig. 1. Reduction assessment and value transformation system for agricultural NPS**  
 89 **loading.** The solid thick arrows indicate the degree of influence or the process output. The thin  
 90 arrows indicate the process input.

## 91 2. Materials and methods

### 92 2.1 Huntai River Watershed

93 The HTRW (40°27'~42°19'N, 121°57'~125°20'E) is situated in the Liaoning province (Northeast  
 94 China), and the river basin area is  $2.73 \times 10^4 \text{ km}^2$ , which comprises approximately 1/5 of the Liaoning  
 95 province (Fig. 2). The HTRW is a tributary of the Liaohe River (one of China's larger water systems)  
 96 and consists of the Hunhe, Taizi, and Daliao Rivers. The Taizi River, Hunhe River, and Daliao River  
 97 watersheds are the HTRW's sub-catchments. The HTRW varies topographically with low mountains  
 98 in the eastern portion and alluvial plains in the other areas. The northeast region has a high elevation.  
 99 Loamy soils are mainly distributed in the alluvial plain, and the average slope in the lower HTRW is

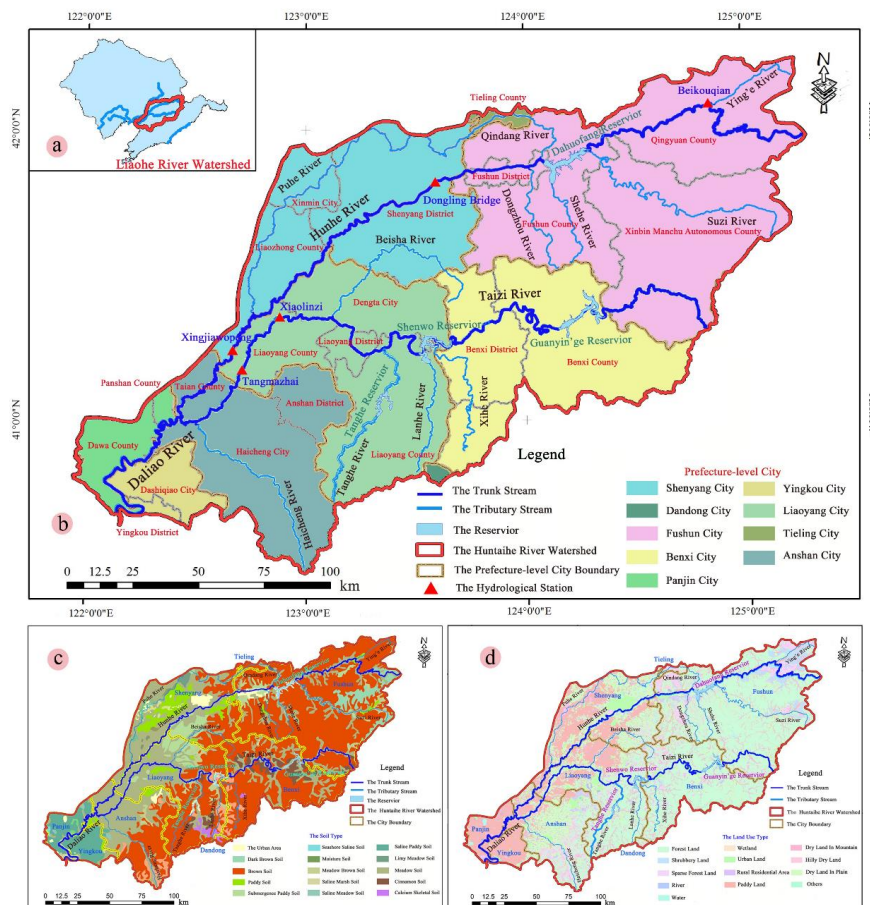


100 approximately 7%. The HTRW area consists of the cities of Shenyang, Fushun, Liaoyang, Anshan,  
101 Benxi, and Yingkou, most of Panjin city. Stream flow and nutrients were measured on five monitoring  
102 stations: Beikouqian, Dongling Bridge and Xingjiawopeng in the Hunhe River and Xialinzi and  
103 Tangmazhai in the Taizi River. HTRW has a temperate continental climate with an average annual  
104 temperature of 7°C and precipitation of 748 mm.

105 The HTRW is in a conventional agricultural farming (farming-dominated products), with  
106 much of the farmland dominated by crops. The total farmland area is 10,763 km<sup>2</sup> (39% of the  
107 total area), including 4,086 km<sup>2</sup> of paddy fields (dominated by rice) and 6,677 km<sup>2</sup> of dry  
108 farmland (including corn, soybean, vegetables and other crops). The upper Hunhe and Taizi  
109 river areas are mountains (69%), plainlands (25%) and low hills (6%). The HTRW's economic  
110 output value is dominated by agricultural cultivation. The farmland is mainly distributed in the  
111 alluvial plain area and valleys in riverine belts. Considering land use, pollutant sources and  
112 rainfall, the HTRW faces a high risk of agricultural pollution. Heavy fertilizer use and soil  
113 erosion in the upper HTRW has led to its heavy water pollution. For example, the Dahuofang  
114 reservoir (located in the middle reaches of Hunhe River) and the water resources-environment  
115 conservation area in its upper sections are facing serious threats, and the agricultural NPS  
116 pollution is becoming increasingly severe with no effective controls. Fertilization in the HTRW  
117 is predominantly nitrogen, followed by potassium and phosphorous. Heavy use of chemical  
118 fertilizers includes mainly DAP (diammonium phosphate), urea and a small amount of N-P-K  
119 (nitrogen-phosphorus-potassium mixed fertilizer). Acetochlor and Atrazine are mainly used on  
120 dryland, and Butachlor is mostly used in paddy soil. Based on 2006-2012 statistical information,  
121 the fertilizer and pesticide quantities (such as Methamidophos and Plifenate) used in the  
122 watershed fluctuated annually. The upper portions of the Huntai and Taizi Rivers are dominated



123 by mountains, and the crops are cultivated and harvested by hand. We obtained these data and  
 124 information, which would normally be inaccessible, through onsite investigations, inquiry visits,  
 125 case studies, example analyses. At present, farmland weeds and pests are mainly controlled by  
 126 pesticides and herbicides. The upstream is rich in forest resources, and the downstream has a  
 127 large amount of farmland. Special landscape layout makes the HTRW a potential area for  
 128 agricultural NPS pollution.



a. The location of the HTRW.

b. The geographical zoning of HTRW.

c. The land use type of HTRW.

d. The soil type of HTRW.



130 **Fig. 2.** Basic HTRW information. The figure was supplied by [www.geodata.cn](http://www.geodata.cn), which is a  
131 national science and technology basic conditions platform and an earth system science data  
132 sharing platform. The figure information is public. The Liaoning province Water Resources  
133 Administrative Bureau granted permission for the basic information on the HTRW.

## 134 **2.2 Setting the scene**

135 To determine the correlation between land use types and agricultural NPS pollutant loading, the  
136 numerical analysis and comprehensive comparison method was used for different land use types  
137 under ecological development and urbanization. In this study, two scenarios were developed: The  
138 status quo scenario (SQS) and the environmental protection scenarios (EPS).

139 The SQS was draw up based on the current environmental protection mode and  
140 socioeconomic developmental structure. The land-use was based on the existing development  
141 pattern and environmental protection policies. BMPs information and environment-friendly  
142 land-use patterns (amount of pesticide and fertilizer used, cultivated land area, and crop species)  
143 were gained from Liaoning Province statistical yearbooks-2013 and field surveys of land  
144 consolidation.

145 The EPS was defined as considering the regional developmental prospects, eco-friendly  
146 environment restoration strategy of the HTRW. Buffer zones were defined as One kilometer  
147 within both banks of the Hunhe, Taizi and Daliao rivers and 5 km around the reservoirs. In the  
148 buffer zones, traditional land-use patterns were changed to restore the natural landscape (forest  
149 and grassland) and ecological environment. This scenario is not only expected to preserve the  
150 fundamental agricultural position in the watershed but also to improve the watershed's  
151 ecosystem service value and biodiversity by reducing the amount of fertilizers and pesticides  
152 used for agricultural productivity. These scenarios can provide a scientific basis for further  
153 understanding characteristics of the nitrogen and phosphorus loading characteristics and



154 cultivated field plantation potential adjustment in HTRW.

155 To simulate the hydrological characteristics by SWAT, we first divided the HTRW into a set  
156 of sub-basins based on DEM data. We then divided sub-basins into Hydrological Response  
157 Units (HRUs). Hunhe River, Taizi River, and Daliao River sub-catchments were delineated into  
158 DEM and river system and further divided by 29 small calculation modules based on 184 HRUs.  
159 We used the monitored data to calibrate and validate the stream flow and pollutant  
160 concentration changes in the HTRW. The land development patterns in the two scenarios were  
161 then input to the SWAT model to simulate the TN and TP pollutant loading. Finally, the spatial  
162 dynamics and ecological service value assessment in NPS pollution loading was analysed based  
163 on land-use. We also analyzed the negative correlation between the agro-ecological value and  
164 the farmland area.

165 The wastewater pollutant source is along both channels of the Taizi, Hunhe, and Daliao River  
166 trunk streams. The risk of NPS pollution is mainly related to the patterns of farmland use and  
167 agricultural planting. The secondary region for water pollution is mainly along the HTRW  
168 tributaries. Therefore, we paid special attention to the comparative analysis of pollutants  
169 generated by the cultivated field adjacent to the water channels.

## 170 **2.3 Methods**

### 171 **2.3.1. SWAT principle**

172 SWAT is a semi-physical and distributed hydrological model developed to quantitatively  
173 predict the responsivity of water quality and quantity to land-use and environmental protection  
174 methods on a watershed scale (Gassman et al.,2007). The primary data imported to run the  
175 model includes soil type, vegetation status/land landscape, DEM (Digital Elevation  
176 Model)/topography, and BMPs. The watershed SWAT model's computing units are the sub-



177 watershed scale and HRUs. Hydrological response unit demarcation is based on land use,  
178 vegetation coverage, soil classification, and different underlying surfaces status.

179 SWAT HRUs are automatically divided by geomorphological features, land development  
180 intensity change, DEM, and soil conditions. To calculate the HRUs, we selected 0% land use,  
181 slope/elevation, and soil classification/attributes as the initial value on the HTRW scale.  
182 Therefore, 184 HRUs were delineated to determine NPS pollutant loading. HRUs are the  
183 minimum units for predicting pollutant output loading, which is automatically generated by  
184 superimposing land-use and soil types within the sub-river basin. Due to the HTRW's large  
185 area and widely changing terrain slope, the HTRW was divided into three levels with slopes of  
186 10 and 30 nodes. The area threshold percentages for land use, soil and slope were 5%, 8%, and  
187 15%, respectively. To evaluate pollutant loss and spatial characteristics, the soil nutrient loss  
188 curve, water-salt balance equation, and stage-discharge curve were applied. Meteorological  
189 data (such as rainfall and wind speed) were gained from automatic weather stations and  
190 hydrological station network in 12 cities within the HTRW. BMP data, such as crop irrigation  
191 time and water, crop harvesting period, fertilizer recovery efficiency, fertilizer dosage, and  
192 spatial layout of the overall land use planning were obtained from environmental and  
193 agricultural management departments or collected by current questionnaire survey.

194 SWAT is mostly used to evaluate N and P pollutants production, diffusion and movement,  
195 and transformation. These pollutions whole process control occur simultaneously with the soil  
196 erosion, hydrological cycle and reasonable utilization of land resource. SWAT considers 5  
197 forms of N and 6 forms of P. The N and P cycles contain mineralization, decomposition,  
198 solidification/stabilization, and conversion. The NPS pollutant loading function is the basis for  
199 evaluating N and P distribution, transportation and transformation (Zhang, 2005). Organic N



200 and P loss was calculated by SWAT by the comprehensive evaluation model of the NPS  
201 pollutant loading, variations of nutrient elements and salt contents of soil, soil environment,  
202 crop growth, and crop yield. The total amount of nitrate lost in the soil was calculated by the  
203 multiplication of water volume and nitrate concentration in the water. Water volume consisted  
204 of groundwater runoff, surface runoff, and interflow/subsurface flow/groundwater recession  
205 flow. The soluble P removed in the runoff was estimated using the P concentration in the soil  
206 partitioning coefficient, surface soil layer, and runoff volume. The concentration of soluble P  
207 in the water was calculated by topsoil P stocks, runoff variation and influencing factors, soluble  
208 P ratio, and soil particle-size characteristics.

209 Surface runoff from daily rainfall data and land use in HRU/sub-basin were calculated and  
210 evaluated using the SCS-CN method. Using the SCS-CN curve, vertical distribution  
211 characteristics and temporal stability of soil water, runoff module number of the ground water,  
212 Soil saturated water content movement and hydraulic conductivity were determined, as well as  
213 the related parameters for daily rainfall. The total discharge temporal variations of runoff from  
214 sub-basin/HRUs is the dynamic equilibrium of groundwater runoff flow, surface runoff flow,  
215 and interflow/subsurface flow. The main routes for water cycle simulation in the SWAT follow  
216 either the network-node mode or the natural-artificial dualistic water cycle mode in river basins  
217 under changing conditions. We used the dualistic mode SWAT flow varies with the dynamic  
218 changes in infiltration, evaporation, transport, and nutrient cycling (Arnold et al.,1998). Direct  
219 runoff is surface runoff resulting from rainfall, which includes surface and return flows.  
220 Baseflow is part of the groundwater recharge to river runoff. Most of the base flow and direct  
221 runoff separation methods are performed by mathematical methods. We used Digital-Filter-  
222 Equation to divide the base flow:



$$\begin{cases} q_t = \beta \cdot q_{t-1} + \alpha(1 + \beta)(Q_t - Q_{t-1}) \\ b_t = Q_t - q_t \end{cases} \quad (1)$$

224 Here,  $q_t$  is the surface runoff at time  $t$ ;  $Q_t$  is the total runoff at time  $t$ ;  $b_t$  is the base flow at time  $t$ ;  
225 and  $\alpha$   $\beta$  are filter parameters.

226 Digital filtering is an objective and effective method of base-stream separation. We assigned  
227  $\alpha = 0.5$  and  $\beta = 0.925$  in the HTRW (Arnold & Allen, 1999). The SWAT HRUs used the soil and  
228 water loss factors, hydrodynamic process of soil erosion, and the universal soil loss equation  
229 (MUSLE) to analyse erosion and sediment form, space distribution characteristic and  
230 influencing factor (Williams, 1975). Sediment was routed through channels using Bagnold's  
231 sediment transport equation (Bagnold, 1977). We used a 2009 version of SWAT to calculate the  
232 parameters.

### 233 2.3.2. Model data input

234 DEM, underlying surface status, geomorphology, soil properties, land vegetation,  
235 hydrological and meteorological data (rainfall, evaporation, temperature) were imported into  
236 the SWAT (Niraula et al., 2013). Fig. 3 shows the basic data used in the SWAT model. We used  
237 30×30 grid data (elevation) as the basis for DEM operation. We downloaded the DEM data for  
238 the HTRW location from the SRTM (Shuttle Radar Topography Mission) data pack. These free  
239 data can be obtained from the website, <http://srtm.csi.cgiar.org/SELECTION/inputCoord.asp>.  
240 The DEM was used to extract the study area and analysis the stream network structure in  
241 relation to geomorphologic features. The stream network in the HTRW was extracted using  
242 1:250,000 digital water system data (www.geodata.com) as an auxiliary model to construct the  
243 HTRW stream network model. We delineated land-use types into 27 categories. The main type  
244 of HTRW land use and land cover change is forest (including orchard, 49%), dry land (24%),  
245 rice paddy (15%), urban land (vacant land, 8%), unused land (uncultivated land, 3%) and

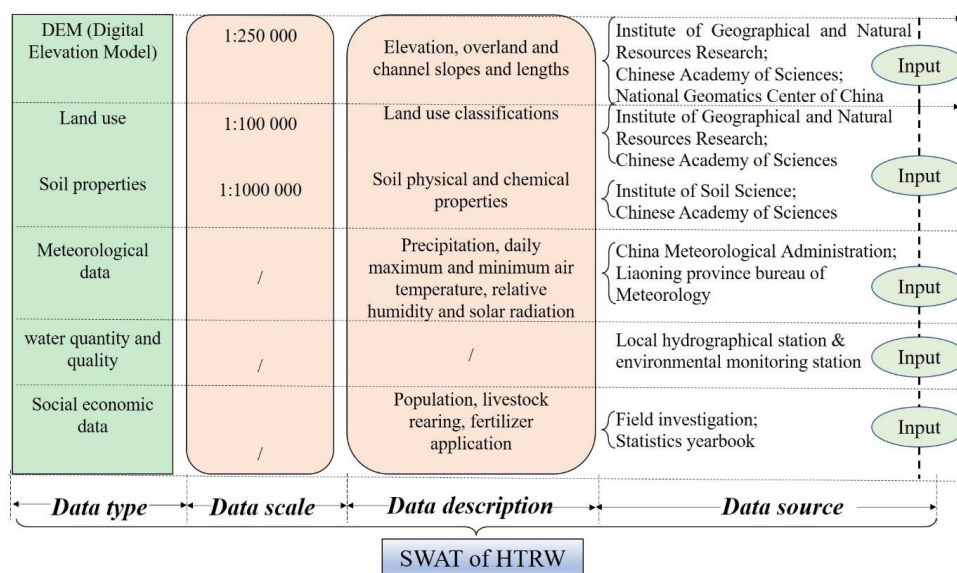


246 grassland (1%). Soil types were classified into 26 types. The primary soil types are brown soil  
247 (54%), meadow soil (30%) and paddy soil (11%). The underlying substrate database was  
248 constructed based on the soil type database using the soil properties and land development data  
249 as underlying substrate parameters (topography characteristics, surface vegetation and soil  
250 types and distribution characteristics). The soil parameters were got from national earth system  
251 science data sharing infrastructure database (<http://www.geodata.cn/aboutus.html>). The  
252 watershed meteorological data used in the current research include rainfall data for 1990-2009  
253 collected by 76 rainfall stations/hydrometric network and hydrometeorological data for 1990-  
254 2009 obtained by 12 city meteorological stations. We used meteorological monitoring data to  
255 simulate rainfall and evaporation. The missing meteorological information can be estimated  
256 using the Long Ashton Research Station Weather Generator (LARSWG-5). At least 3 sets of  
257 water monthly monitoring data for ammonia (NH<sub>3</sub>, NH<sub>4</sub>), nitrite (NO<sub>2</sub>), nitrate (NO<sub>3</sub>), TP, and  
258 TN, were available for 2006–2009. We obtained information on plant species, cropping systems,  
259 sowing time, fertilization time, distribution pattern of soil productivity, and regional economic-  
260 social development from investigations and the statistics department in HTRW. The SWAT  
261 uses the LH-OAT (Latin Hypercube One-factor-At-a-Time) sensitivity analysis method and the  
262 SCE-UA (Shuffled Complex Evolution Algorithm) automatic calibration analysis method to  
263 determine the value of sensitive parameters.

264 Data information (scale, type, description) for SWAT in the HTRW are shown in Fig. 3. We  
265 imported the related soil and meteorological data for SWAT from the China Meteorological  
266 Administration and Environmental-Ecological Science Data Center for West China. The China  
267 Hydrology, Water Resources and Water Quality Monitoring Department of the HTRW  
268 provided the automatic and regular monitoring hydrological data sequence. The Liaoning



269 Province Water Resources Administrative Bureau granted permission for the modelling the  
 270 pollutant generation response to different land utilization scenarios in the HTRW.



271

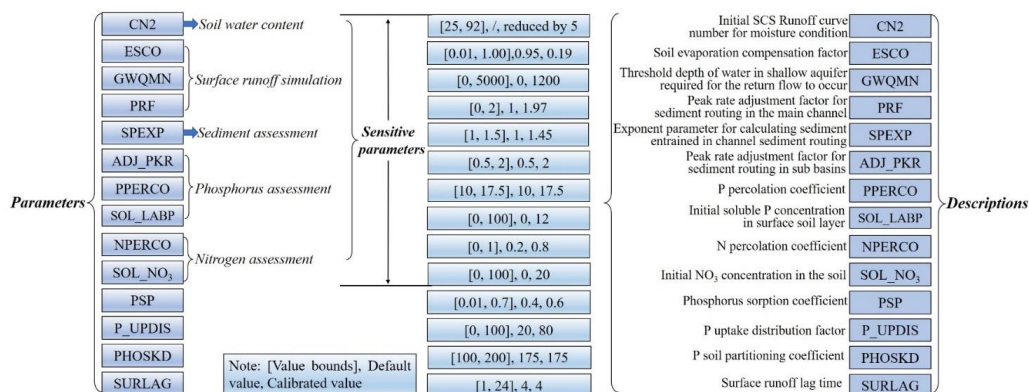
272 **Fig. 3.** HTRW data. The basic data imported into the SWAT model included spatial data and  
 273 attribute data. Spatial data includes DEM, land use and land cover data, soil spatial distribution  
 274 data, digital river network data, and the spatial location of meteorological stations and  
 275 hydrological stations. Attribute data mainly includes land use attribute database, soil type  
 276 attribute database, LARSWG-5 and hydro-meteorological data.

### 277 2.3.3. Calibration and validation

278 The monthly scale data were used to simulate SWAT. We used the open code SWAT-CUP  
 279 module to calibrate the parameters of SWAT in HTRW (Abbaspour et al.,2007). A sequential  
 280 uncertainty fitting algorithm had a higher calculation accuracy and efficiency, which was  
 281 extensively used in the SWAT-CUP module (Wang et al.,2014; Yang et al.,2008). We manually  
 282 input the optimal parameters into the SWAT model for hydrology series simulation. The  $E_{NS}$   
 283 (Nash-Sutcliffe efficiency coefficient),  $Dv$  (relative deviation), and  $R^2$  (certainty coefficient)



284 were used to assess the runoff flow change of the HTRW hydrological station.  
 285 The runoff was calibrated, followed by N, P and other nutrients. The runoff was calibrated  
 286 and tested using monitoring data from the Xingjiawopeng and Tangmazai hydrological stations  
 287 (Fig. 2). The simulated values of N and P were calibrated using on-site monitoring data from  
 288 Dongling bridge, Beikouqian, Xiaolinzi, Xingjiawopeng, and Tangmazhai hydrological  
 289 stations. We automatically calibrated 10 sensitivity parameters, then we applied the SWAT  
 290 manual calibration helper to make small and targeted adjustments to the calibration results to  
 291 improve the simulation accuracy based on auto-calibration results. Various water quality and  
 292 hydrologic parameters (test data) were adjusted under their change interval to fit with the  
 293 monitored/observed data (Fig. 4). GWQMN, SURLAG, and ESCO were three key parameters  
 294 in the calibration and water flow validation (Shen et al., 2010). The other sensitive parameters  
 295 selected for calibration and validation in the HTRW are shown in Fig. 4. In the HTRW, the  
 296 Liaoning Province government began monthly monitoring of pollutants in 2006. The TN and  
 297 TP loading, and runoff data, used for calibration and validation were from 1992 to 2009 and  
 298 from 2006 to 2008, respectively.



300 **Fig. 4.** Calibration of SWAT model parameters in the HTRW. Based on the spatial analysis of



301 sensitive parameters, we analyzed the influencing factors of the parameter values combining  
302 with the underlying surface runoff factors of the basin.

303 In the present study, the simulated effects were evaluated by analyzing and comparing the  
304 runoff hydrograph,  $D_v$ ,  $E_{NS}$  and  $R^2$ . The  $D_v$  was used to simulate the entire water quantity  
305 deviation;  $E_{NS}$  and  $R^2$  were used to simulate the simulation effects (Nash, 1970). The  $D_v$ ,  $E_{NS}$   
306 and  $R^2$  were calculated as

$$307 \quad D_v = [(M - W) / W] \times 100\% \quad (2)$$

308 Here,  $D_v$  was the relative deviation;  $W$  was the observed mean value; and  $M$  was the predicted mean  
309 value.

$$310 \quad E_{NS} = 1 - [\sum_{i=1}^n (W_i - M_i)^2 / \sum_{i=1}^n (W_i - \bar{W})^2] \quad (3)$$

311 Here,  $E_{NS}$  was the Nash-Sutcliffe efficiency coefficient;  $W_i$  was the observed data at the  $i^{th}$   
312 period;  $M_i$  was the simulated data at the  $i^{th}$  period; and  $\bar{W}$  was the observed mean value.

$$313 \quad R^2 = \{[\sum_{i=1}^n (W_i - \bar{W})(M_i - \bar{M})] / [\sqrt{\sum_{i=1}^n (W_i - \bar{W})^2} \sqrt{\sum_{i=1}^n (M_i - \bar{M})^2}]\}^2 \quad (4)$$

314 Here,  $R^2$  was the certainty coefficient;  $W_i$  was the observed value at time  $i$ ;  $M_i$  was the simulated  
315 value at time  $i$ ;  $\bar{W}$  was the observed mean value, and  $\bar{M}$  was the predicted mean value.

316 The first four years (1990-1994) were regarded as the stage for SWAT to minimize the  
317 uncertainty of initial meteorology and underlying surface values. Sensitivity analysis of the  
318 parameters is an effective mean to help assessing impact of uncertainty in the input and  
319 parameters on the output uncertainty. The sensitivity evaluation indicators differed between  
320 SWAT and SWAT-CUP. Student's t-test is used by SWAT-CUP and is part-sensitive. To  
321 improve the model calibration accuracy and verification results, we used SWAT-CUP and the  
322 SUFI-2 algorithm to analyse the parameters' sensitivity. To determine the sensitivity of various



323 parameters, one parameter was auto-adjusted at a time based on the accuracy and change  
324 interval in Fig. 4. To calibrate the stream flow, we subsequently calibrated runoff and nutrients  
325 (TP and TN) with the same geographical and hydrological data. During calibration, we used  $R^2$   
326 and the correlation coefficient of the residual sequence ( $SCR$ ) to eliminate the uncertainties  
327 caused by the differences in water quality sampling and testing methods.

### 328 **3. Results and discussion**

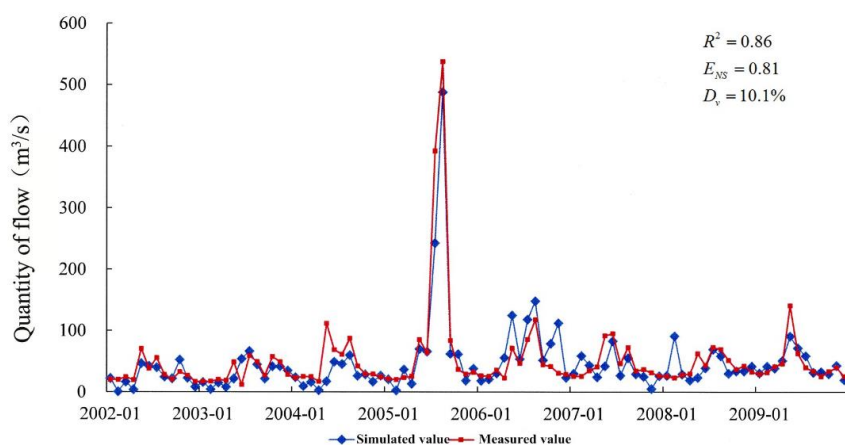
#### 329 **3.1 Modelling validation**

330 **Stream flow.** Because of HTRW lacks basic runoff data, the present study focused on  
331 calibrating and testing the runoff model. First, we dealt with the meteorological data and  
332 retained the 1990-2001 data series, then supplied the meteorological data simulation value from  
333 1990 to 2001 by SWAT. Second, we input the runoff data for 1995-2001 into the SWAT-CUP  
334 model to calibrate the runoff parameters and entered these parameters into the SWAT database,  
335 then extended the meteorological data series to 1990-2009 and simulated runoff again. Finally,  
336 we compared the runoff simulation values with monitoring values from 2002 to 2009. During  
337 annual calibration, the runoff curve data were calibrated and the available water content in the  
338 soil and the soil evaporation compensation coefficient were modified. Finally, the monthly  
339 runoff curve was modified. CN2 is a comprehensive parameter that reflects the watershed  
340 characteristics before rainfall and is mainly affected by the hydrology and soil types, land use,  
341 pre-soil moisture and tillage management measures. CN2 directly affects the surface runoff,  
342 and the larger the CN2 value, the larger the runoff yield. The same land-use type yields greater  
343 permeability with a smaller CN2 value or lower vegetation coverage and rainfall interception  
344 ability with a greater CN2 value. Different HRUs have different CN2 values. The moist area

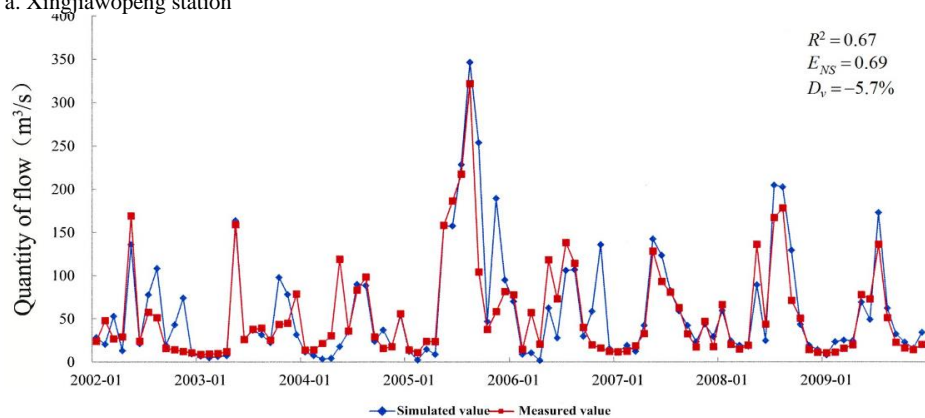


345 (climate division) has the highest CN2 ranging from 60~96, while other regions vary greatly.  
346 Within the same soil types, the CN2 value was the highest for cultivated land, followed by  
347 grassland. Woodland was the lowest. For the simulation, 1990-1994 was the model preparation  
348 period, 1995-2001 was the model calibration period, and 2002-2009 was the model validation  
349 period.

350 For the calibration step,  $E_{NS}$  and  $R^2$  for Xingjiawopeng hydrological station and Tangmazhai  
351 hydrological station were both greater than 0.6, and the  $|Dv|$  values were less than 20% during  
352 the model preparation period, suggesting that the SWAT model parameters were reliable after  
353 calibration. The monitoring value fit better with the simulation value obtained from  
354 hydrographic curve. Most top values observed were highly similar. For the model calibration  
355 period, the matching curves for the simulated and measured monthly runoff values at  
356 Xingjiawopeng and Tangmazhai hydrological stations are shown in Figs. 5(a) and (b). The  
357 runoffs at these two hydrological stations were well matched. However, the accuracy of the  
358 simulated runoff for the second halves of the years 2002, 2005 and 2006 was poor, likely due  
359 to the data series length and specific stations selected. For the simulation and evaluation  
360 standards for the hydrological model, the simulation effects at the monthly scale were much  
361 better.



a. Xingjiawopeng station



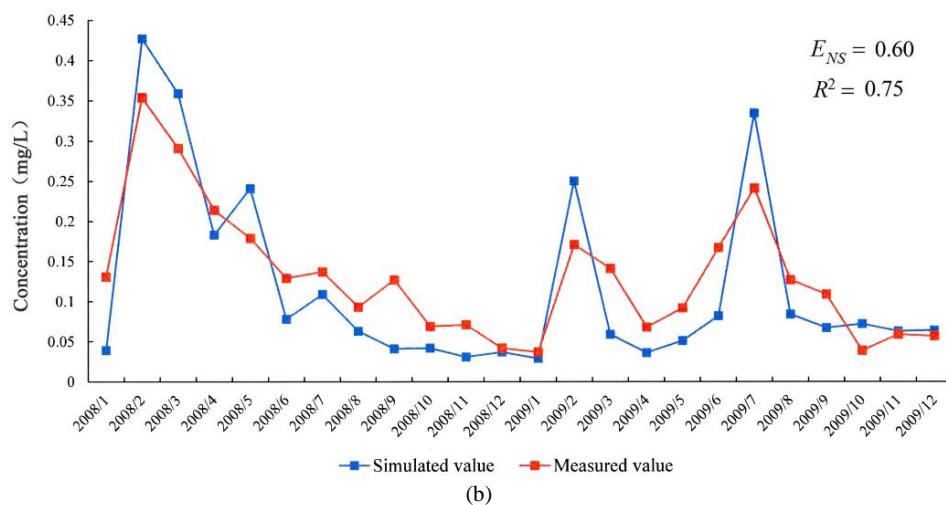
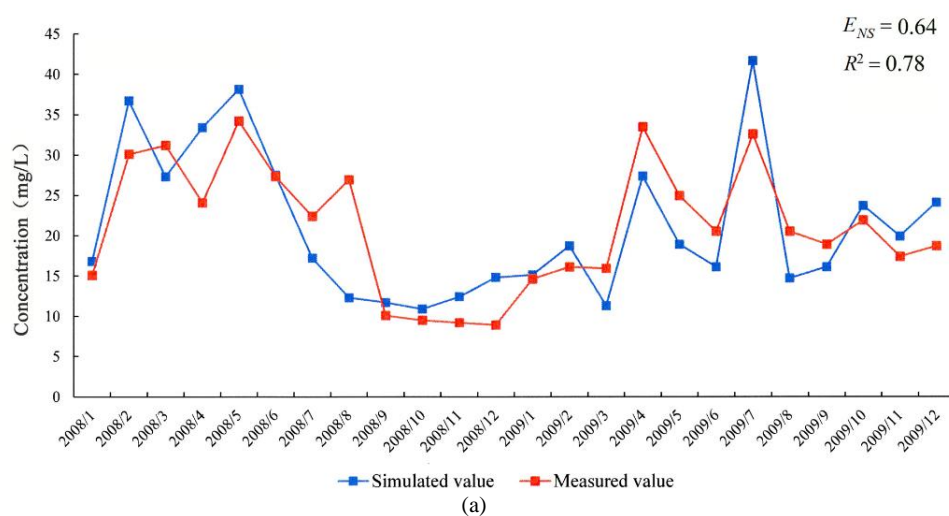
b. Tangmazhai station

362 **Fig. 5.** Stream flow validation of a typical monitoring station.

363 **Nutrients.** The nutrient concentrations in the water were simulated by SWAT. By verifying  
 364 the accuracy of the initial concentrations, the nitrate and soluble P loading can be simulated by  
 365 adjusting the nitrogen permeability coefficient (NPERCO) and the phosphorous permeability  
 366 coefficient (Lam et al., 2011). Beikouqian, Xingjiawopeng, Xiaolinzi and Tangmazhai  
 367 hydrological stations had continuous monthly water quality monitoring data from 2006 to 2007  
 368 (model calibration period). Only the monthly data on TN and TP in Beikouqian were validated  
 369 from 2008 to 2009. The Xingjiawopeng, Xiaolinzi and Tangmazhai Hydrological stations had



370 only the TN data during the study period; therefore, Beikouqian was selected for the validation  
371 curves, and the TN  $E_{NS}$  and  $R^2$  were 0.64 and 0.78, and the TP  $E_{NS}$  and  $R^2$  were 0.60 and 0.75,  
372 respectively (Figs. 6 a and b). The  $E_{NS}$  and  $R^2$  for the Xingjiawopeng, Xiaolinzi and Tangmazhai  
373 hydrological stations were 0.62 and 0.73, 0.61 and 0.72, and 0.62 and 0.77, respectively. The  
374 values of all  $R^2$  were higher than 0.7, confirming that the SWAT could be used for water quality  
375 simulation in HTRW.





376 **Fig. 6.** Nutrient validation at Beikouqian station. Figure (a) and (b) shows the fitting result of  
377 TN and TP, respectively.

### 378 **3.2 NPS pollutant loading under the status quo scenario**

379 The NPS pollutant generation output was calculated using the pollutant loading approach  
380 based on the attributes of the regional calculation results and land-use scenarios in HTRW.  
381 The generated N and P for different calculation units were calculated based on the spatial  
382 changes in soil types, crops and residuals, as well as the differences in the coefficients of N and  
383 P losses under different land uses. The paddy fields, rural residential areas, urban development,  
384 and vegetation type may be important indicators for variability in NPS pollution, and nutrition  
385 pollution was influenced by the integrated effects of different land uses (Cai et al., 2015; Lee et  
386 al.,2010). The annual generated TN and TP were 18,707 t and 53,322 t, respectively (Table  
387 1). Brown soil is widely distributed in the HTRW. We supplied the N and P loss  
388 characteristics under different land-use types and fertilization, as shown in Table 2 (Hao,  
389 2012). The brown soil thickness was 30-50 cm in HTRW. The organic content, TN and TP  
390 decreased significantly with the soil depth increment. Nutrients were mainly found in soils  
391 of 0-30 cm deep, where TN and TP reserves reached more than 50% of the total soil reserves.  
392 Large-scale use of fertilizers (DAP, N:46.4% and N-P-K, N:15%; P<sub>2</sub>O<sub>5</sub>:15%; K<sub>2</sub>O:15%) and  
393 livestock and poultry excrement (N:0.5-0.6%; P:0.45-0.6%; K:0.35-0.5%) were the important  
394 sources of agricultural NPS pollution. In HTRW, the number of pastures and cattle was small,  
395 and cattle excrement was collected and processed by the farmer. The excessive or unreasonable  
396 application of fertilizers and the fertilizer utilization rate were not high (the utilization rate of  
397 nitrogen is 30% to 60% and of phosphorus is 2% to 25%), resulting in substantial fertilizer loss.  
398 The nutrient content (mainly from agricultural production activities) of the soil (20cm below



399 the surface) in the HTRW was 1.21 t/ha. Information on initial soil nutrient content and  
 400 fertilizers was used for model parameterization.

401 **Table 1.** Pollutant generation in the HTRW under the status quo scenario

Watershed	Area (km <sup>2</sup> )	Run off (E+08 m <sup>3</sup> )	Pollutant (t)			Pollutant loading (kg/ha)		
			Sediment	TP	TN	Sediment	TP	TN
Hunhe River	11,565	24.04	220,004	8,993	24,264	190	8	21
Taizi River	13,903	33.31	1,699,996	6,399	19,010	1,223	5	14
Daliao River	1,913	1.60	300,002	3,315	10,048	1,568	17	53
Total/Average	27,381	58.95	2,220,002	18,707	53,322	811	7	19

402 Source: China Hydrology; national earth system data sharing infrastructure; field investigation of Liaoning  
 403 province; chemical fertilizer/land area/soil erosion statistics yearbook of Liaoning province; Liaoning  
 404 province Bureau of Meteorology.

405 **Table 2.** Loss characteristics of N and P under different land uses and fertilization

Land use	Soil thickness (cm)	Organic matter content (g/kg)	Unit weight of soil (g/cm <sup>3</sup> )	Soil particle composition (mm)			TN (g/kg)	TP (g/kg)
				Clay $\phi \leq 0.002$	Loam $0.002 < \phi \leq 0.005$	Sand $0.005 < \phi \leq 2$		
Cultivated field	0-5	24.58	1.42	21.05	57.35	21.6	0.96	0.47
	5-30	18.45	1.48	24.71	24.71	18.84	0.88	0.38
	0-5	27.6	1.18	15.97	15.97	14.58	1.25	0.58
Grassland	5-30	21.75	1.25	20.36	20.36	21.5	1.02	0.42

### 406 3.2.1. Sediment

407 Sediment loading is the data basis for calculating TN and TP loading and is affected by the  
 408 type of land development and vegetation coverage (generally dominated by forest and  
 409 farmland). Based on the SWAT model simulation, the annual sediment outputs generated in the  
 410 Hunhe, Taizi and Daliao River watersheds were  $22 \times 10^4$  t,  $170 \times 10^4$  t and  $30 \times 10^4$  t, respectively.  
 411 The annual soil erosion loading in HTRW was 0.811 t/ha, and its spatial distribution is shown  
 412 in Fig. 7(a). The soil erosion value varied widely in different regions, with the change interval  
 413 from 0 to 2 t/ha. Soil erosion in the Daliao River watershed was severe (up to 2 t/ha in some



414 regions), followed by the Taizi River watershed (1 t/ha in most regions) and the Hunhe River  
415 watershed (less than 0.2 t/ha in most regions). Yingkou and Dashiqiao have even topography,  
416 and incoming silt from the upper areas is accumulated therein. The soil erosion modulus is  
417 therefore very high, which contributes greatly to the silt input to the HTRW. The soil erosion  
418 was affected by natural and human factors. The natural factors mainly included topography,  
419 underlying surface conditions and soil type. The human factors mainly consisted of vegetation  
420 coverage, precipitation, land use, crop cultivation and cultivated land farming methods.  
421 Moreover, mountainous areas have great soil erosion (Hong et al.,2012). The Daliao River had  
422 a large cultivated land area; therefore, soil erosion was more likely. Soil types are also key  
423 influencing factors in causing soil erosion; therefore, brown and paddy soils are prone to  
424 accumulating sediment (Hong et al.,2012).

### 425 **3.2.2. TP**

426 From the SWAT simulation results, the annual TP output generated in the Hunhe, Taizi and  
427 Daliao River watersheds was 8993 t, 6399 t and 3315 t, respectively, and the HTRW output  
428 loading was 7 kg/ha. The TP loading had the same spatial distribution pattern as the sediment  
429 loading, ranging from 0 to 260 kg/ha. Fig. 7(b) shows the TP spatial variation loading of the  
430 HTRW. A large amount of P could be deposited in the downstream plain. The changes in the  
431 TP loading were affected by topography, precipitation, land use, and silt losses. The TP output  
432 loading on the Daliao River watershed slope was higher than that of the Hunhe River watershed,  
433 while the Taizi River watershed was the lowest. Many fertilizers and pesticides have been  
434 applied to the farmland, and organophosphate pesticides accounted for 40% of the total  
435 pesticides (Wang, 2012). The paddy fields, brown soil and dry lands were mainly distributed in  
436 the Hunhe River downstream. Therefore, the P loading in these plains areas was higher (Li et



437 al., 2010). Correspondingly, the cities and counties with large proportions of farmland have  
438 higher TP output loading, such as Dashiqiao, Panshan and Dawa city in the Daliao River  
439 watershed and the city of Haicheng and Taian county in the Hunhe River watershed. Regions  
440 with large proportions of developed land have lower TP output loading, including the city centre  
441 of Fushun, Shenyang in the Hunhe River watershed, the municipal districts of Liaoyang city  
442 and Benxi city at the Taizi River watershed. Based on land use, tributaries with higher  
443 proportions of farmland have the highest TP output loading, while tributaries with substantial  
444 vegetation cover as forested land have relatively lower TP output loading. TP output loading is  
445 closely related to soil characteristics and attributes.

### 446 **3.2.3. TN**

447 Simulation and calculation results showed that the TN generation output in the Hunhe, Taizi  
448 and Daliao River watersheds was 24264 t, 19010 t and 10048 t. The annual TN output loading  
449 in the watershed was 19 kg/ha. Fig. 7(c) shows the spatial variation of TN loading in the HTRW.  
450 The TN loading interval varied from 0.001 to 365 kg/ha. The TN loading had the same spatial  
451 characteristics as TP loading. The TN output loading in the Daliao River watershed was greater  
452 than that in the Hunhe River watershed, while the Taizi River watershed was the lowest. Large  
453 amounts of fertilizer were applied in the study area. Nitrate and organic N accounted for a  
454 substantial portion of the fertilizer used in HTRW. Therefore, the TN output loading in the  
455 watershed was very high. Regions with much farmland, such as the middle and lower portions  
456 of the Hunhe River, the lower portions of the Taizi River and the tributaries in the upper portions  
457 of the Daliao River, have high TN output loading. The organic N contents in the forested land  
458 were very low. Thus, the output loading of TN in regions with high vegetation forest cover,  
459 such as the mountainous areas in the upper parts of the Taizi and Hunhe rivers, was very low.

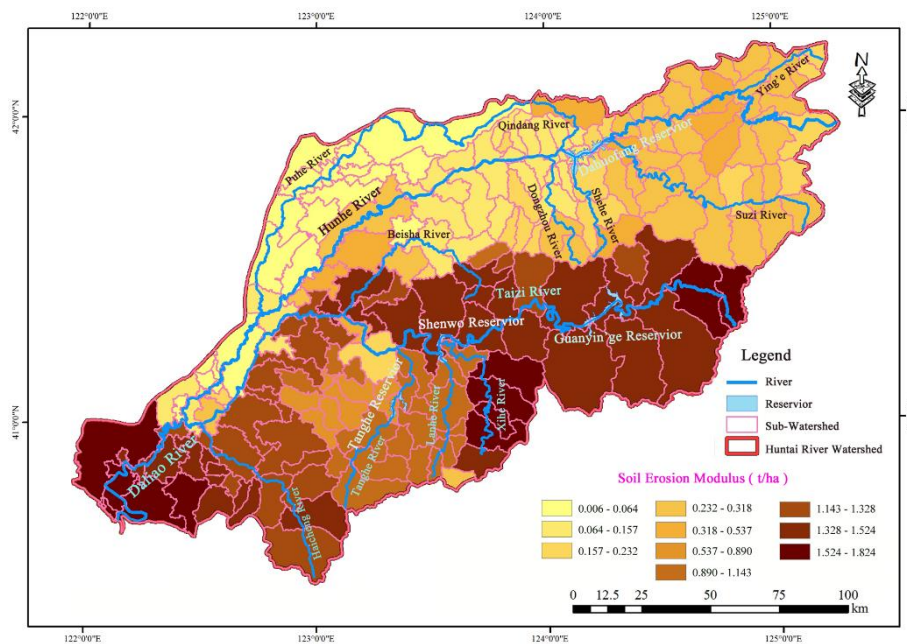


460 The TN output loading in municipal districts with highly developed areas was the lowest, such  
461 as in the municipal districts of Fushun city and Shenyang city in the Hunhe River watershed  
462 and the municipal districts of Benxi city, Liaoyang city and Shenyang city in the Taizi River  
463 watershed.

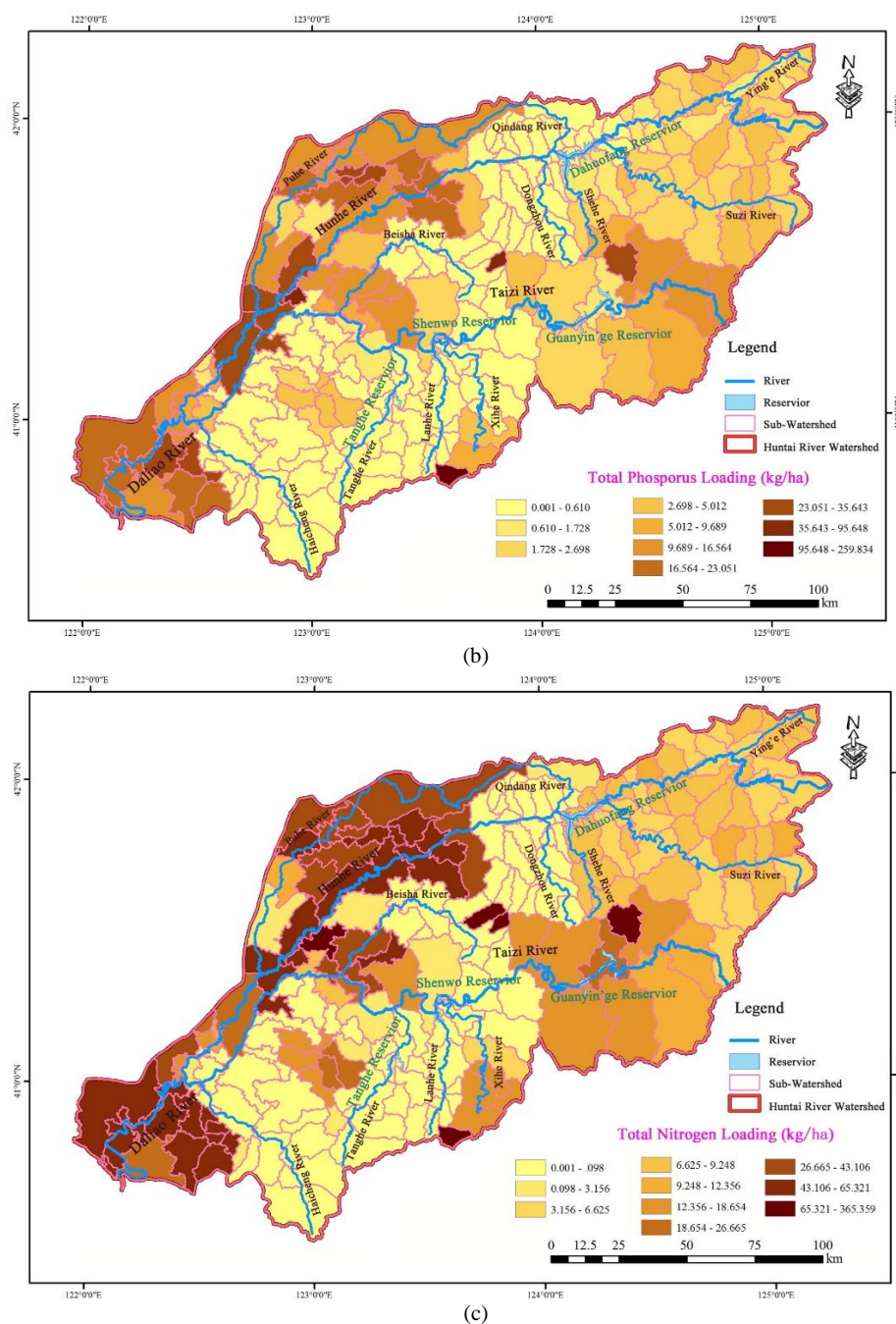
464 TN and TP loading in the HTRW were characterized by a regional distribution. Although  
465 Qingyuan, Yibin and Benxi counties, located in the upper areas of the HTRW, had high water  
466 and silt output, their pollutant loading was low. Per unit area, the maximum TN and TP loading  
467 (maximized over space) was 365 and 260 kg/ha, respectively. The regions TN and TP with high  
468 loading were mainly distributed in Taian, Haicheng, and Fushun city. The TP and TN loading  
469 near the Dahuofang, Tanghe, Shenwo and Tanghe reservoirs were low, ranging from 0.006 to  
470 10 kg/ha and from 0.08 to 19 kg/ha, respectively. Based on topography and soil distribution,  
471 the slope is very steep in the upper stream of HTRW. The soils are predominately brown soil  
472 and salted paddy soil, both of which are easily eroded. The topography in the lower sections is  
473 usually flat, such as in the cities of Anshan, Haicheng, Yingkou and Panjin. The elevation is  
474 low, and the soil is predominately meadow soil and brown soil, both of which have higher soil  
475 erosion rates, silt loss and output loading of pollutants. The regions with heavy TN and TP  
476 loading included Xinmin county, located in the middle and lower reaches of the HTRW, the  
477 municipal district of Shenyang city, Liaozhong county, Dengta city, Liaoyang county, the  
478 municipal district of Anshan city, Haicheng city and a portion of Dashiqiao city. Based on the  
479 land development pattern in the Taizi River, dry fields and paddy fields were mainly distributed  
480 on the plain areas of this watershed, which constitute therefore a core source of output loading.  
481 The spatial differences in the TN and TP loading were no large differences. Based on  
482 topography, landform, soil types and land development status in the watershed, the upper



483 streams of the watershed have high vegetation coverage, less farmland and low pollutant  
 484 loading, while the lower areas have more farmland, high fertilizer application rates and high  
 485 soil erosion and pollution loading (Yin et al., 2011). In summary, the spatial characteristics of  
 486 TN loading resulted from comprehensive effects of precipitation/runoff characteristics, soil  
 487 properties, soil erosion and vegetation coverage. Therefore, to effectively control TN loading  
 488 and soil erosion in the HTRW, the BMPs, fallow measures of cultivated fields, watershed  
 489 vegetation restoration and soil and water conservation in the upper stream are the most  
 490 important measures to implement.



(a)



491 **Fig. 7.** NPS pollution loading distributions of HTRW under the status quo scenario. The Figure



492 (a), (b) and (c) showed the loading distributions of contaminant sediment, TN and TP,  
493 respectively.

### 494 **3.3 NPS pollutant loading under EPS**

495 There exists a correlation between land development mode and water environment  
496 protection and rehabilitation at the basin scale. The riparian buffer zones effectively reduced  
497 the concentration levels of  $\text{NO}_3^-$  in the water, which were 47% lower than those of the soil  
498 content. Dry farmland caused higher NPS pollutant loading, followed by paddy lands, rural  
499 and urban areas, forestland, and shrub lands. Hence, under the EPS, the farmland area in the  
500 watershed was reduced. A modest area of farmland (29,500 ha, accounting for 3% of the total  
501 farmland area) was converted to forestland (including shrub land, 14,753 ha; grassland, 5,899  
502 ha; and wetland, 8,848 ha), while NPS pollution from farmland decreased. The water quality  
503 protection objective within the watershed's critical zoning was realized. The riparian buffers  
504 can be planted in various diverse vegetations. The N removal rate of a 60-m-wide woody soil  
505 buffer zone was 16% and 38% higher than that of shrubbery and grassland, respectively.  
506 Approximately 1 kilometre within both banks of the Hunhe, Taizi and Daliao river tributaries  
507 and 5 kilometres of surrounding reservoirs buffer zones were defined, including 1946 km<sup>2</sup> of  
508 farmland, urban land, and rural residential land. This accounts for 7% of the total area in the  
509 watershed. The woodland coverage rate was reduced by 1%, and the loading of sediment, TP and  
510 TN increased by 0.01-11, 0.2-3 and 0.4-14 kg/km<sup>2</sup>, respectively. The pollutant generation output  
511 under EPS was calculated by transforming the existing land-use type.

512 The TN and TP respective ranges of change were 0 to 365 kg/ha and 0 to 260 kg/ha. The  
513 annual losses of TN and TP were reduced by 13,839 and 1,946 t/yr., respectively. In comparison,  
514 the NPS pollutant generation output under the EPS was decreased by 22% compared with that



515 under the SQS, whereas the TP and TN outputs were reduced by 10% and 26%, respectively.  
 516 Under the EPS, the average loading of TN and TP was 14 and 6 kg/ha on a unit area basis,  
 517 which were 14% and 26% less than the loading under the SQS, respectively. The NPS pollutant  
 518 loading declined in the EPS. The variation of TP and TN pollutant loading between the SQS  
 519 and EPS is shown in Table 3. The amount of change indicated that riparian buffer and land  
 520 development pattern change effectively reduced NPS pollutant loading in the HTRW.

521 **Table 3.** Loading variation in TP and TN pollutant between EPS and the status quo scenario

Watershed	Pollutant loading of EPS (kg/ha)		Pollutant loading variation (kg/ha)		Farmland variation (ha)	Forestland variation (ha)	Grassland variation (ha)	Wetland variation (ha)	Pollutant annual variation(t/yr.)	
	TP	TN	TP	TN					TP	TN
Hunhe River	7	16	-1	-5	-12,460	+6,231	+2,492	+3,737	-838	-5,743
Taizi River	4	10	-1	-4	-14,979	+7,491	+2,995	+4,493	-776	-5,606
Daliao River	16	40	-1	-13	-2,061	+1,031	+412	+618	-332	-2,490
Total/Average	6	14	-1	-5	-29,500	+14,753	+5,899	+8,848	-1,946	-13,839

522 “—” denotes a decrease compared to that of the status quo scenario; “+” denotes an increase compared to  
 523 that of the status quo scenario.

### 524 3.4 Value transformation based on NPS pollutant loading

525 Based on the results of Simpson (2014), the correlation between the yield, input of land,  
 526 purchase investment, ecosystem services value, and land area is expressed as

$$527 \quad q = f(x, S, A) \quad (6)$$

528 where  $q$  is the yield,  $x$  is the quantity of the purchase investment,  $S$  is the quantity of the  
 529 supplied ecosystem services,  $A$  is the land area directly utilized for agricultural production.

530 Formula (6) is a conceptual formula, and there is no sole unit for each letter in formula (6).

531 To obtain a general expression, we give a special instance of production function.

$$532 \quad q = f(x, S, A) = x^\alpha S^{1-\alpha} - \gamma(x^\alpha S^{1-\alpha})^2 / A \quad (7)$$

533 Where  $\alpha=1/2$ ,  $\gamma$  was a positive constant.

534 The constant profit of a massive production function is expressed as (Vincent & Binkley,  
 535 1993)



$$536 \quad q = \sqrt{x \cdot S} - \gamma \cdot x \cdot S / A \quad (8)$$

537 This is a simple production function with limitations. Assuming that  $r$  represents the price of  
538 the input. When the price of the yield is normalized as 1, the profit  $\eta$  is expressed as

$$539 \quad \eta = \sqrt{x \cdot S} - \gamma \cdot x \cdot S / A - r \cdot x \quad (9)$$

540 For  $x$ , the first-order condition for maximal profit is expressed as

$$541 \quad \begin{cases} \frac{1}{2} \sqrt{S/x} - \gamma \cdot S / A - r = 0 \\ -\frac{\varphi}{2} \sqrt{x/S} + \gamma \cdot x \cdot \frac{\varphi \cdot \bar{A}}{A^2} = 0 \end{cases} \quad (10)$$

542 and when the first-order of Eq. (10) is satisfied, the second-order condition for maximal  
543 management was also satisfied. After the conversion, we obtained

$$544 \quad x = \frac{S}{4(\gamma \cdot S / A + r)^2} \quad A = \frac{\bar{A}}{1 + \sqrt{r / \gamma \cdot \varphi}} \quad (11)$$

545 The ecosystem services of the preserved land were determined by the parameter,  $\varphi$ . In the  
546 production function, ecosystem services and the purchase investment were the substitute items.  
547 When the purchase price increases, the area of the land used for production will decrease,  
548 suggesting that more land should be preserved. When more land is preserved for maximal profit,  
549 the yield will decrease. When Eq. (10) was multiplied by  $x$ , we obtained

$$550 \quad \frac{1}{2} \sqrt{x \cdot S} - \gamma \cdot x \cdot S / A - r \cdot x = \eta - \frac{1}{2} \sqrt{x \cdot S} = 0 \quad (12)$$

551 where the total differential of Eq. (12) was calculated concerning  $A$ . If  $A$  and  $x$  were used to  
552 realize maximal profits, the arithmetic resolution could be calculated as

$$553 \quad \frac{dx/x}{dA/A} = \frac{A}{A-A} \quad (13)$$

554 therefore, when most of the land was used for production, the dependence on the purchase  
555 investment increased. If more land was used in agricultural production activities, greater costs



556 would be paid to compensate for lost ecosystem services. If the initial consideration was the  
 557 excessive dependence on purchase investments, the margin rate of technically replacing the  
 558 purchase investment by ecosystem services increased, indicating that the purchase investment  
 559 would be reduced significantly.

560 If the land area used for agricultural production was changed, profits ( $\partial q/\partial x=r$ ) were  
 561 maximized by

$$562 \quad \frac{dq/q}{dA/A} = \frac{r \cdot x}{q} \frac{A}{A-A} \quad (14)$$

563 If the agricultural production was dependent on the purchase investment in the current  
 564 watershed to a greater degree, a significant yield reduction would occur.

565 The total value of the water and soil conservation, material investment, and service  
 566 investment was calculated using the energy price per unit of land area in the river basin as a  
 567 reference (Fu et al., 2017). The agricultural production investment value in HTRW was  
 568 calculated indirectly by the equivalent conversion between the investment and the acquired  
 569 value. The cost investment for agricultural production in HTRW was ¥ 217.13 E+08  
 570 (USD\$ 34.12 E+08) (Table 4).

571 **Table 4.** Energy prices of agricultural production in HTRW (based on status quo scenario).

Classification	Details	Energy value (Sej/ha)	Price of energy (¥/ha)	Total values (¥ E+08)	Cost investment (¥ E+08)
Water and soil conservation	Soil erosion	3.08E+14	594.53	6.40	6.40
	Depreciation	3.05E+15	1,960.34	21.10	21.10
Material investment	Fuel oil	2.90E+13	18.64	0.20	0.20
	Material	1.42E+16	9,126.83	98.23	98.23
	Labour	1.29E+16	8,291.28	89.24	89.24
Service investment	Maintenance and management	2.51E+14	161.33	1.74	1.74
	Service	3.30E+13	21.21	0.23	0.23
<i>Total</i>				217.13	217.13

572 To calculate the elasticity of the farmland yield data derived from Eq. (13), the expression  
 573 was used as follows:



574 
$$\left(\frac{dq}{q}\right) / \left(\frac{dA}{A}\right) = \left(\frac{217.13E+08}{3800E+08}\right) / \left(\frac{29500}{1076300}\right) = 2. \quad (15)$$

575 Here,  $dq$  was the farmland production cost after deducting the paid amount,  $q$  was the  
576 agricultural production value of the farmland,  $dA$  was the total reduced area of the farmland  
577 under EPS, and  $A$  was the total area of the farmland. We obtained the agricultural production  
578 value from Liaoning Province statistical yearbooks-2013.

579 Based on this calculation, to maximize profit, 1% of the currently cultivated or used land in  
580 HTRW was converted into preserved land to supply more ecosystem services. Accordingly, the  
581 crop yield in HTRW was reduced by 2%. The analysis results based on the ecological land-use  
582 value in HTRW, the forestland, grassland, and wetlands were the main suppliers of ecosystem  
583 services. Therefore, the decreased farmland and increased the ecological value of the non-  
584 cultivated land were profit indicators.

## 585 4. Conclusions

586 NPS pollution often occurs on dry farmlands and in paddy, rural and urban areas. Many  
587 studies have applied the SWAT model to study NPS in China, mainly focusing on scenario  
588 simulations of NPS pollution and management in agricultural areas with rich hydrological and  
589 meteorological data. Basic monitoring data on HTRW were deficient. Thus, we selected SWAT  
590 as a feasible method for assessing NPS pollutant loading at the watershed level. We applied  
591 specific practices based on EPS to reduce NPS pollutant loading in the Hunhe, Taizi and Daliao  
592 River watersheds. The status quo scenario and EPS were used to calculate the NPS pollutant  
593 generation output. NPS pollutant generation output and TN and TP loading were reduced by  
594 22%, 26% and 10% compared with that of the SQS, respectively. The crop yield was reduced  
595 by 2% when the land area for ecosystem services in the basin increased by 1%.



596 The SWAT model can calculate the potential reduction of agricultural NPS pollutants based  
597 on different land uses. The reliability of SWAT evaluation results are decided by information  
598 completeness and the reasonable degree of parameter initialization. To determine pollutant  
599 reduction under different land development patterns and examine the uncertainty of  
600 sensitivity parameters, the SWAT model in China has many potential applications.  
601 Considering the significance of ecosystem services, much attention should be paid to the  
602 relationship between ecosystem service increases and crop yield decreases. Only in this way  
603 can ecosystem services and land use be harmoniously developed.

## 604 **Acknowledgements**

605 The study was financially supported by the National Key Research and Development Program  
606 of China (2016YFC0401408), Comprehensive Regulation Theory and Application of Basin  
607 Water Environment Process (WE0145B532017) and Project Based Personnel Exchange  
608 Program with China Scholarship Council & German Academic Exchange Service of 2015.

## 609 **References**

- 610 Abbaspour, K.C., Yang, J., Maximov, I., Siber, R., Bogner, K.: Modelling hydrology and water quality in the  
611 pre-alpine/alpine Thur watershed using SWAT, *J. Hydrol.*, 333, 413-430, 2007.
- 612 Ahearn, D.S., Sheibley, R.W., Dahlgren, R.A.: Land use and land cover influence on water quality in the last  
613 free flowing river draining the western Sierra Nevada, California, *J. Hydrol.*, 313, 234-247, 2005.
- 614 Arnold, J., Allen, P.: Automated Methods for Estimating Baseflow and Ground Water Recharge from  
615 Streamflow Records. *Journal of the American Water Resources Association*, 35, 411-424, 1999.
- 616 Arnold, J.G., Srinivasan, R., Muttiah, R.S.: Large area hydrologic modelling and assessment. Part I: Model  
617 development, *Journal of the American Water Resources Association*, 34, 73-89, 1998.
- 618 Cai, Y., Zhao, D.H., Xu, D.L., Jiang, H., Yu, M.Q.: Influences of Land Use on Sediment Pollution across  
619 Multiple Spatial Scales in Taihu Basin, *Clean-Soil, Air, Water*, 43, 1616-1622, 2015.
- 620 Department of Environmental Protection of Liaoning Province: Liaoning Province Environmental Bulletin,  
621 2011.
- 622 Ficklin, D.L., Luo, Y.Z., Luedeling, E., Zhang, M.H.: Climate change sensitivity assessment of a highly



- 623 agricultural watershed using SWAT, *J. Hydrol.*, 374, 16-29, 2009.
- 624 Fu, Y.C., Du, X., Ruan, B.Q, Liu, L.S., Zhang, J. Agro-ecological compensation of watershed based on  
625 emergy. *Water Science & Technology*, 76, 2830-2841. 2017.
- 626 Gassman, P.W., Reyes, M.R., Green, C.H., Arnold, J.G.: The Soil and Water Assessment Tool: Historical  
627 development, applications and future directions, *Trans ASABE*, 50, 1211-1250, 2007.
- 628 Gosain, A.K., Rao, S., Srinivasan, R.: Return-flow assessment for irrigation command in the Palleru River  
629 Basin using SWAT model, *Hydrol Process*, 19, 673-682, 2005.
- 630 Hao, L.P.: Characteristics of nitrogen and phosphorus losses of rainfall runoff in Liaoning Hunhe Basin,  
631 Shenyang Agricultural University, 2012.
- 632 Hong, Q., Sun, Z., Chen, L., Liu, R., Shen, Z.: Small-scale watershed extended method for nonpoint source  
633 pollution estimation in part of the Three Gorges Reservoir Region, *Int J Environ Sci Technol.*, 9, 595-  
634 604, 2012.
- 635 Lam, Q.D., Schmalz, B., Fohrer, N.: The impact of agricultural Best Management Practices on water quality  
636 in a North German lowland catchment, *Environ Monit Assess*, 183, 351-379, 2011.
- 637 Lee, M.S., Park, G.A., Park, M.J.: Evaluation of non-point source pollution reduction by applying Best  
638 Management Practices using a SWAT model and Quick Bird high resolution satellite imagery, *Journal*  
639 *of Environmental Sciences*, 22, 826-833, 2010.
- 640 Li, M., Zhu, B., Hou, Y.L.: Phosphorus release risk on a calcareous purple soil in southwest China, *Int J*  
641 *Environ Pollut.*, 40, 351-362, 2007.
- 642 Liu, M., Li, C.L., Hu, Y.M., Sun, F.Y.: Combining CLUE-S and SWAT Models to Forecast Land Use Change  
643 and Non-Point Source Pollution Impact at a Watershed Scale in Liaoning Province, China. *Chin. Geogra.*  
644 *Sci.*, 24, 540-550, 2014.
- 645 Logsdon, R.A., Chaubey, I.: A quantitative approach to evaluating ecosystem services, *Ecological Modelling*,  
646 257, 57-65, 2013.
- 647 Nash, J.E., Sutcliffe, J.V.: River flow forecasting through conceptual models part I-A discussion of principles,  
648 *J Hydrol.*, 10, 282-290, 1970.
- 649 Niraula, R., Kalin, L., Srivastava, P., Anderson, C.J.: Identifying critical source areas of nonpoint source  
650 pollution with SWAT and GWLF, *Ecological Modelling*, 268, 123-133, 2013.
- 651 Outram, F.N., Cooper, R.J., S`unnenberg, G., Hiscock, K.M., Lovett, A.A.: Antecedent conditions,  
652 hydrological connectivity and anthropogenic inputs: factors affecting nitrate and phosphorus transfers  
653 to agricultural headwater streams, *Sci Total Environ.*, 545, 184-199, 2016.
- 654 Ouyang, W., Huang, H., Hao, F.: Synergistic impacts of land-use change and soil property variation on non-  
655 point source nitrogen pollution in a freeze-thaw area, *J. Hydrol.*, 495, 126-134, 2013.
- 656 Ouyang, W., Wang, X., Hao, F.: Temporal-spatial dynamics of vegetation variation on non-point source  
657 nutrient pollution, *Ecological Modelling*, 220, 2702-2713, 2009.



- 658 Robinson, T.H., Leydecker, A., Keller, A.A.: Steps towards modeling nutrient export in coastal Californian  
659 streams with a Mediterranean climate, *Agricultural Water Management*, 77, 144-158, 2005.
- 660 Sadeghi, S.H.R., Jalili, K., Nikkani, D.: Land use optimization in watershed scale, *Land Use Policy*, 26, 186-  
661 193, 2009.
- 662 Shen, Z.Y., Chen, L., Hong, Q.b., Qiu, J.L.: Assessment of nitrogen and phosphorus loads and causal factors  
663 from different land use and soil types in the Three Gorges Reservoir Area, *Sci Total Environ.*, 454, 383-  
664 392, 2013.
- 665 Shen, Z.Y., Hong, Q., Yu, H., Niu, J.F.: Parameter uncertainty analysis of non-point source pollution from  
666 different land use type, *Sci Total Environ.*, 408, 1971-1978, 2010.
- 667 Shen, Z.Y., Liao, Q., Hong, Q., Gong, Y.W.: An overview of research on agricultural non-point sources  
668 pollution modelling in China, *Sep Purif Technol.*, 9, 595-604, 2011.
- 669 Simpson, R.D. Ecosystem services as substitute inputs: basic results and important implications for  
670 conservation policy. *Ecol Econ.* 98, 102-108. 2014.
- 671 Vincent, J. R., Binkley, C.S., 1993. Efficient multiple-use forestry may require land-use specialization. *Land*  
672 *Econ.* 69, 370-376.
- 673 Wang, G., Yang, H., Wang, L., Xu, Z., Xue, B.: Using the SWAT model to assess impacts of land use changes  
674 on runoff generation in headwaters, *Hydrol Process*, 28, 1032-1042, 2014.
- 675 Wang, X.L., Wang, Q., Wu, C.Q., Liang, T., Zheng, D.H., Wei, X.F.: A method coupled with remote sensing  
676 data to evaluate non-point source pollution in the Xin'anjiang catchment of China, *Sci Total Environ.*,  
677 430, 132-143, 2012.
- 678 Williams, J.R.: Sediment routing for agricultural watersheds, *Water Resour. Bull.*, 11, 965-974, 1975.
- 679 Yang, J., Reichert, P., Abbaspour, K.C., Xia, J., Yang, H.: Comparing uncertainty analysis techniques for a  
680 SWAT application to the Chaohe Basin in China, *J Hydrol.*, 358, 1-23, 2008.
- 681 Yang, J.L., Zhang, G.L., Zhao, Y.G.: Land use impact on nitrogen discharge by stream: a case study in  
682 subtropical hilly region of China, *Nutrient Cycling in Agroecosystems*, 77, 29-38, 2007.
- 683 Yang, Y., Wang, G., Wang, L., Yu, J., Xu, Z.: Evaluation of Gridded Precipitation Data for Driving SWAT  
684 Model in Area Upstream of Three Gorges Reservoir, *PLOS ONE*, 9, e112725. doi:  
685 10.1371/journal.pone.0112725, 2014.
- 686 Yin, G., Wang, N., Yuan, X.: Non-point source pollution of nitrogen and phosphorus nutrients using SWAT  
687 model in tumen river watershed, China, *Journal of Agro-Environment Science*, 30, 704-710, 2011.
- 688 Zhang, Y.H.: Development of Study on Model-SWAT and Its Application, *Progress in Geography*, 24, 121-  
689 130, 2005.